

Investigation of N₂O Production from 266 and 532 nm Laser Flash Photolysis of O₃/N₂/O₂ Mixtures

E. G. Estupiñán,[†] J. M. Nicovich,[‡] J. Li,[†] D. M. Cunnold,[†] and P. H. Wine^{*,†,‡}

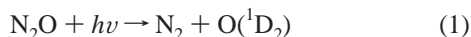
School of Earth and Atmospheric Sciences and School of Chemistry and Biochemistry,
Georgia Institute of Technology, Atlanta, Georgia 30332

Received: November 15, 2001; In Final Form: April 1, 2002

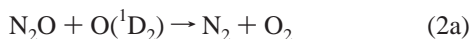
Tunable diode laser absorption spectroscopy has been employed to measure the amount of N₂O produced from laser flash photolysis of O₃/N₂/O₂ mixtures at 266 and 532 nm. In the 532 nm photolysis experiments very little N₂O is observed, thus allowing an upper limit yield of 7×10^{-8} to be established for the process $O_3^{\ddagger} + N_2 \rightarrow N_2O + O_2$, where O_3^{\ddagger} is nascent O₃ that is newly formed via $O(^3P_J) + O_2$ recombination (with vibrational excitation near the dissociation energy of O₃). The measured upper limit yield is a factor of ~ 600 smaller than a previous literature value and is approximately a factor of 10 below the threshold for atmospheric importance. In the 266 nm photolysis experiments, significant N₂O production is observed and the N₂O quantum yield is found to increase linearly with pressure over the range 100–900 Torr in air bath gas. The source of N₂O in the 266 nm photolysis experiments is believed to be the addition reaction $O(^1D_2) + N_2 + M \xrightarrow{k_6} N_2O + M$, although reaction of (very short-lived) electronically excited O₃ with N₂ cannot be ruled out by the available data. Assuming that all observed N₂O comes from the $O(^1D_2) + N_2 + M$ reaction, the following expression describes the temperature dependence of k_6 (in its third-order low-pressure limit) that is consistent with the N₂O yield data: $k_6 = (2.8 \pm 0.1) \times 10^{-36} (T/300)^{-(0.88 \pm 0.36)} \text{ cm}^6 \text{ molecule}^{-2} \text{ s}^{-1}$, where the uncertainties are 2σ and represent precision only. The accuracy of the reported rate coefficients at the 95% confidence level is estimated to be 30–40% depending on the temperature. Model calculations suggest that gas phase processes initiated by ozone absorption of a UV photon represent about 1.4% of the currently estimated global source strength of atmospheric N₂O. However, these processes could account for a significant fraction of the oxygen mass-independent enrichment observed in atmospheric N₂O, and they appear to be the first suggested photochemical mechanism that is capable of explaining the altitude dependence of the observed mass-independent isotopic signature.

1. Introduction

Nitrous oxide (N₂O) is a climatically important species affecting the Earth's radiation budget. Its contribution to the greenhouse effect is considerable due to its long residence time of 120 ± 30 years¹ and its relatively large energy absorption capacity per molecule.² On a per molecule basis, N₂O is estimated to be 296 times more powerful than CO₂ as a greenhouse gas (based on 100 year global warming potentials).³ Nitrous oxide is inert in the troposphere. However, in the stratosphere, especially in the middle and upper stratosphere, N₂O is destroyed by photolysis ($\lambda \sim 180\text{--}215$ nm):



Process 1 accounts for $\sim 90\%$ of photochemical N₂O destruction.¹ The other 10% of N₂O photochemical loss is via reaction with $O(^1D_2)$:⁴



About 40% of the $N_2O + O(^1D_2)$ reaction proceeds via channel

2a and about 60% via channel 2b.⁴ Reaction 2b represents the dominant source of total reactive nitrogen (NO_y) in the stratosphere.^{5,6}

The global atmospheric N₂O budget is the least well-constrained of the major greenhouse gas budgets. Well-documented major sources all introduce N₂O into the atmosphere near the Earth's surface, and include soils under natural vegetation, oceans, agricultural activities, combustion, and biomass burning.³ Even though considerable progress has been made in recent years in the identification of new sources, the uncertainties associated with individual sources have not been reduced (i.e., $\pm 50\%$ or larger). Recent estimates of the global N₂O source strength range from 7 to 37 Tg of N₂O per year,^{3,7–9} with a "best guess" value of ~ 16 Tg of N₂O per year. The possible existence of in situ atmospheric sources of N₂O is still a controversial subject, although laboratory studies are reported in the literature that provide evidence for the existence of such sources.^{10–12} In addition, recent isotopic studies have cast doubts on the current understanding of the global N₂O budget. One important aspect that these studies have revealed is that atmospheric N₂O samples show a mass-independent heavy oxygen isotope effect, i.e., an anomalous ratio of N₂¹⁷O-to-N₂¹⁸O concentration ratio, which increases with altitude (or distance from known sources).^{13,14} Calculations by Miller and Yung^{15,16} predict that N₂O UV photolysis in the stratosphere selectively destroys "light N₂O", thus leaving behind N₂O that is enriched in the heavier isotopes of both N and O. Recent laboratory

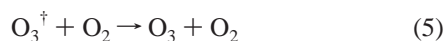
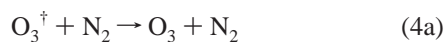
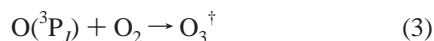
* To whom correspondence should be addressed at School of Chemistry and Biochemistry. E-mail: pw7@prism.gatech.edu.

[†] School of Earth and Atmospheric Sciences.

[‡] School of Chemistry and Biochemistry.

experiments^{17–21} support the predictions of Miller and Yung, and recent field observations^{21–23} are also consistent with the magnitude of the enrichments in ¹⁴N¹⁴N¹⁸O, ¹⁴N¹⁵N¹⁶O, and ¹⁵N¹⁴N¹⁶O predicted by the Miller and Yung theory. However, N₂O photolysis is a mass-dependent process^{14,16} and, therefore, does not account for the mass-independent fractionation in N₂O.

The research described in this paper was initiated to evaluate the possible formation of N₂O from the interaction of nascent (highly vibrationally excited) O₃ (O_{3[†]}) with N₂ in N₂ + O₂ buffer gas:



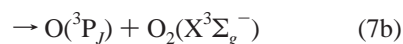
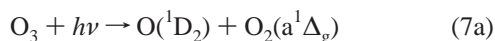
As described by Cliff and Thieme, ¹³O₃ is an ideal candidate as the source of mass-independently isotopically enriched N₂O in the atmosphere. Laboratory studies of reaction 3 have shown that O₃ formation is accompanied by mass-independent enrichment, i.e., δ¹⁷O ≈ δ¹⁸O ≈ 85%.²⁴ In addition, measurements of both stratospheric O₃^{25,26} and tropospheric O₃^{27,28} have shown extraordinarily large O₂¹⁷O excesses (compared to the mass-dependent O₂¹⁷O/O₂¹⁸O ratio), Δ¹⁷O, ranging from about 22‰ to 35‰.^{26–28} Reaction 4b would result in a direct transfer of mass-independently enriched oxygen to N₂O, and thus, it could provide a possible explanation for the observed atmospheric isotopic signature of N₂O.^{13,14}

Our study of reaction 4b has also been motivated by the work of Zipf and Prasad¹² and Prasad and Zipf,²⁹ who report an N₂O yield, $k_{4b}[\text{N}_2]/\{(k_{4a} + k_{4b})[\text{N}_2] + k_5[\text{O}_2]\}$, of 4×10^{-5} in air at pressures of 1–1000 Torr, which translates into an atmospheric annual production rate of about 6 Tg of N₂O per year,²⁹ i.e., nearly 40% of the “best guess” N₂O source strength.^{3,7–9} The laboratory work by Zipf and Prasad¹² suggests that either the N₂O surface sources have been *largely* overestimated or the atmospheric sinks have been *largely* underestimated. In addition, a source of the magnitude described by Zipf and Prasad¹² may not be consistent with the small, but readily observed ¹⁷O excess of Δ¹⁷O ≈ 1‰ in atmospheric N₂O.^{13,14,30} Therefore, one of the major goals of our work has been to resolve the above inconsistencies and firmly establish the role of reaction 4b in the atmospheric N₂O budget. Our experimental technique minimizes potential complications and uses a nonintrusive spectroscopic technique to detect N₂O.

Motivated by results of preliminary experiments, and by the large range of rate coefficients reported in three previous studies of reaction 6^{31–33}



we have also carried out a temperature-dependent study of N₂O production resulting from 266 nm photodissociation of O₃/N₂/O₂ mixtures (which we believe results from the occurrence of reaction 6). It is important to point out that since O(¹D₂) is generated from the photolysis of O₃



reaction 6 (like reaction 4b) would also constitute a direct transfer of mass-independently enriched oxygen atoms to N₂O. Hence, reaction 7a followed by reaction 6 warrants careful investigation.

2. Experimental Technique

The laser flash photolysis (LFP)—tunable diode laser absorption spectroscopy (TDLAS) apparatus used in this study was similar to systems previously employed in this laboratory to study the production of N₂O from reactions of electronically excited NO₂³⁴ and OH³⁵ with N₂. Schematic diagrams of similar versions of the detection system are shown in the cited publications.^{34,35} As a result, only the important features related to this study are presented here.

Three sets of experiments were carried out. These are labeled as preliminary experiments, 532 nm irradiation experiments (designed to study the N₂O yield from nascent O₃ deactivation in N₂ + O₂ buffer gas), and temperature-dependent 266 nm irradiation experiments (designed to evaluate the rate coefficient for reaction 6 as a function of temperature and pressure). Experimental details related to each individual set of experiments are discussed in separate sections below.

2.1. Preliminary Experiments. O(³P_{*j*}) atoms were produced by 266 nm laser flash photolysis of mixtures containing typically 0.1–0.3 Torr of O₃ in synthetic air buffer gas in a static cell equipped with antireflection (AR) coated quartz windows (248–355 nm). TDLAS in a connected multipass cell with internal mirrors was used for N₂O detection.

A Quanta Ray Nd:YAG laser (Model DCR-2A, pulse width ~6 ns) operating at a frequency of 10 Hz served as the photolytic source. At λ = 266 nm, the yield of O(¹D₂) from O₃ photodissociation is known to be 0.88 and the yield of O(³P_{*j*}) is known to be 0.12.³⁶ Most of the experiments were performed in a Pyrex reaction cell with an internal volume of ~580 cm³, while two experiments were performed using a Pyrex cylindrical cell 15 mm in diameter and 50 cm in length with a smaller internal volume (~95 cm³). O₃ was introduced into the photolysis cell by expanding O₃ (with some residual O₂) from a silica gel trap held at 195 K. This trap was used to collect O₃ prepared by passing O₂ through a commercial ozonator. Synthetic air was introduced into the photolysis cell directly from its high-pressure tank.

The incoming Nd:YAG laser power was monitored by a silicon photodiode (cross-calibrated against a disk calorimeter) positioned near the entrance of the reaction cell. A thin, glass optic was used to pick off a portion of the laser beam and direct it onto the photodiode, which was equipped with a stack of thin Teflon diffusers to prevent saturation. The laser power exiting the reaction cell was monitored by a Scientech Model 214 disk calorimeter.

The concentration of O₃ in the reaction cell was monitored by UV photometry at 253.7 nm (Hg penray lamp light source). The lamp radiation crossed the reaction cell perpendicular to the direction of the laser beam through two additional quartz windows positioned near the center of the reaction cell. Placing a narrow aperture between the Hg penray lamp and the window of the reaction cell minimized O₃ photolysis by the lamp. A band-pass filter isolated the 253.7 nm Hg line (in a region of strong O₃ absorption, i.e., σ(253.7 nm) = 1.144 × 10⁻¹⁷ cm² molecule⁻¹^{37–42}), and a UV-sensitive photomultiplier tube monitored the light level. Blank experiments with the lamp on and the photolysis laser blocked were used to confirm that N₂O production from lamp-induced photochemistry was negligible.

The number of $O(^3P_J)$ atoms generated per laser pulse was calculated from the incoming laser power (corrected for window losses), the fraction of laser photons absorbed by the O_3 molecules in the reaction cell, and the estimated quantum yield of $O(^3P_J)$ from the chemistry taking place in the reaction cell (i.e., 2.0 ± 0.3). The fraction of laser photons absorbed by the O_3 molecules was computed from the measured O_3 concentration, the laser path length through the photolysis cell, and the known room-temperature absorption cross section of O_3 at 266 nm (i.e., $9.49 \times 10^{-18} \text{ cm}^2 \text{ molecule}^{-1}$).³⁹ Measurement of the incoming and exiting radiation ("dual beam" absorption measurement) permitted a second, more direct, evaluation of the fraction of laser photons absorbed by the O_3 molecules in the reaction cell.

Nitrous oxide was monitored at 2207 cm^{-1} using highly monochromatic infrared radiation from a lead salt tunable diode laser housed in a liquid nitrogen Dewar. The pressure in the photolysis cell, the Hg lamp intensity, and the ratio of the two digitized first harmonic signals from the IR detection system were all digitized and fed into an MS-DOS compatible microcomputer, where information was stored for later analysis.

2.2. 532 nm Irradiation Experiments. The experimental system used was similar to the one employed in the preliminary 266 nm experiments. Only the differences are discussed below.

$O(^3P_J)$ atoms were produced by 532 nm laser flash photolysis of mixtures containing typically 1 Torr of O_3 in synthetic air buffer gas in a static cell equipped with quartz windows. The reaction cell was a Pyrex cylinder 15 mm in diameter and 50 cm in length with O-ring joints for attaching windows (internal volume $\sim 95 \text{ cm}^3$). A Quanta Ray Nd:YAG laser (Model DCR-2A, pulse width $\sim 6 \text{ ns}$) operating at a frequency of 10 Hz served as the photolytic source. The laser power exiting the reaction cell (typically 95 mJ/pulse) was monitored by a Scientech Model 214 disk calorimeter. The corrected (for window losses) exiting laser power could be used as a measure of the incoming laser photons since at 532 nm and 1 Torr of O_3 less than 0.5% of the laser radiation is absorbed by the O_3 molecules in the reaction cell. The number of $O(^3P_J)$ atoms generated per laser pulse was calculated from the incoming laser power, the fraction of laser photons absorbed by the O_3 molecules in the reaction cell, and the known $O(^3P_J)$ yield of unity at 532 nm.⁴³

2.3. Temperature-Dependent 266 nm Irradiation Experiments. The experimental apparatus used to study reaction 6 was almost identical to the one used in the preliminary experiments. Only a slightly different reaction cell was employed. The cell was a Pyrex cylinder 15 mm in diameter and 50 cm in length with O-ring joints for attaching antireflection (AR) coated quartz windows (248–355 nm) (internal volume $\sim 100 \text{ cm}^3$). The cell was maintained at constant temperature by circulating ethylene glycol ($T > 298$) or methanol ($T < 298$) from a thermostated bath through the outer jacket. A copper–constantan thermocouple with a stainless steel jacket was inserted into the center of the reaction cell to measure the gas temperature under the precise pressure conditions of the experiment. The temperature measurement was made after all the kinetic experiments were performed simulating the same bath and pressure conditions as during the actual experiments.

The O_2 used in this study was Ultra Pure Carrier Grade with a minimum purity of 99.996%. Synthetic air was UHP/Zero Grade with stated total hydrocarbon and water contents of less than 0.5 and 3.5 ppm, respectively. The N_2O calibration gas was a certified standard containing 0.969 ppmv N_2O in UHP N_2 . All three gases were used as supplied.

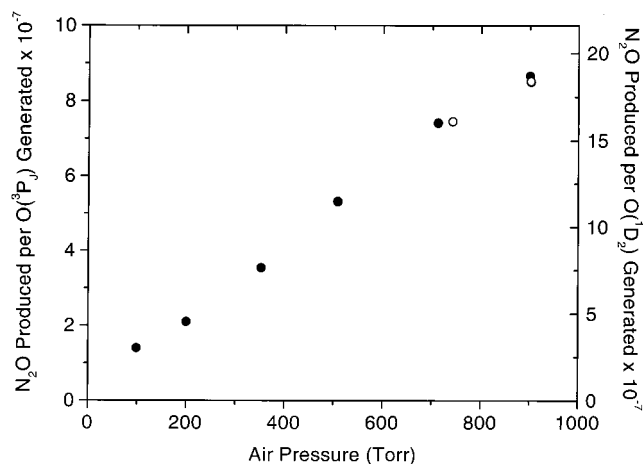


Figure 1. Plot of number of N_2O molecules detected per $O(^3P_J)$ atom generated (left axis) and number of N_2O molecules detected per $O(^1D_2)$ atom generated (right axis) as a function of air pressure. Filled circles indicate experiments performed in a $\sim 580 \text{ cm}^3$ volume reaction cell, and empty circles indicate experiments performed in a $\sim 95 \text{ cm}^3$ volume reaction cell.

3. Results and Discussion

3.1. Preliminary Experiments. All the experiments were carried out under static-fill conditions. The first set of experiments was designed to test the possibility that N_2O could be generated by background sources ("blank" experiments). Three 1 h irradiations at 266 nm were performed at 100, 500, and 900 Torr total pressure of air (no O_3 present). In addition, two O_3 /air mixtures (i.e., 0.1 and 0.3 Torr of O_3) at total pressures of 500 and 900 Torr, respectively, were allowed to remain in the photolysis cell for periods of 1 h (i.e., typical irradiation times) with the Hg lamp on but the laser blocked. In all five cases, when the photolysis products were expanded into the infrared cell, negligible, if any, N_2O was detected.

The second set of experiments was designed to determine the number of N_2O molecules produced per $O(^3P_J)$ atom generated. Figure 1 shows the results of these experiments. Readily detectable N_2O yields were measured, and the yields were observed to increase linearly with pressure. However, the N_2O yields depicted in Figure 1 are about 2 orders of magnitude lower than the N_2O yield reported by Zipf and Prasad.¹² Three possible interpretations of the results of these preliminary experiments are possible. The first interpretation is that the N_2O yield from the reaction of nascent O_3 with N_2 is about a factor of 100 smaller than the one measured by Zipf and Prasad.¹² The second interpretation is that the observed N_2O results from some other process (for example, the addition of electronically excited oxygen atoms ($O(^1D_2)$) to N_2) and, therefore, the yield of N_2O from the reaction of nascent O_3 with N_2 is negligibly small. It is important to point out that if the yield of N_2O from the reaction of nascent O_3 with N_2 had turned out to be of the order reported by Zipf and Prasad,¹² then the N_2O resulting from other sources would have made a negligible contribution to the total number of N_2O molecules detected. The third interpretation is, of course, that two or more processes are contributing a significant fraction of the total number of N_2O molecules detected at the end of the experiment.

In an attempt to decide if the second interpretation was feasible, the number of $O(^1D_2)$ atoms generated in each experiment were integrated and a second N_2O yield was calculated (i.e., the number of N_2O molecules detected per $O(^1D_2)$ atom generated; right axis of Figure 1). Preliminary calculations indicated that, in this scenario, the room-temperature

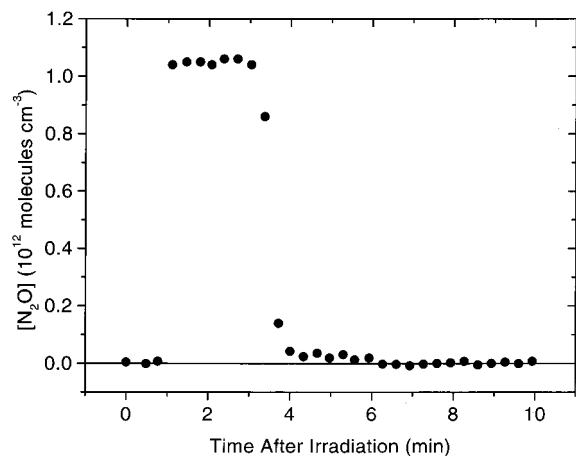


Figure 2. Plot showing the time history of N₂O absorption measurements made after the irradiation in experiment 2 (Table 1). Details of the experimental procedure and data interpretation are given in the text.

rate coefficient for reaction 6 would be about $25 \times 10^{-37} \text{ cm}^6 \text{ molecule}^{-2} \text{ s}^{-1}$. In fact, some agreement exists between this preliminary value and the three previously published studies of reaction 6. Our preliminary room-temperature rate coefficient is a factor of 3–7 larger than two literature values^{32,33} but within 10% of the room-temperature rate coefficient reported by Gaedtker et al.³¹ In addition, the observed linear dependence of the N₂O yield on pressure seems consistent with the expected behavior of reaction 6 in the low-pressure third-order regime. Both the magnitude of the observed N₂O yield and the pressure dependence of the observed N₂O yield are, therefore, consistent with the possibility that the observed N₂O is coming from reaction 6.

3.2. 532 nm Irradiation Experiments. To shed some light on the first possible interpretation discussed above, the reaction of nascent O₃ with N₂ was studied by irradiating O₃/air mixtures with radiation that only yields O(³P_J) atoms from the photolysis of O₃ (i.e., 532 nm). This set of experiments was designed to completely eliminate the possible interference from reaction 6 to the observed N₂O yield and, thus, definitively assess the role of reaction 4b in the N₂O budget. However, to detect an N₂O yield of the order presented in Figure 1, or even lower, we were forced to slightly change our experimental apparatus and initial conditions. At 532 nm, the yield of O(³P_J) from the photolysis of O₃ is unity⁴³ (compared to the estimated O(³P_J) yield of 2.0 ± 0.3 in the 266 nm irradiations) and, more critically, the O₃ absorption cross section is only $2.65 \times 10^{-21} \text{ cm}^2 \text{ molecule}^{-1}$ (about a factor of 3600 lower than at 266 nm).⁴⁴ As a result, to generate a detectable level of N₂O, this new set of experiments were carried out, as briefly pointed out in the Experimental Section, in a smaller volume reaction cell ($\sim 95 \text{ cm}^3$) and with a higher initial O₃ concentration ($\sim 1 \text{ Torr}$). Furthermore, irradiations were allowed to proceed for 10 h.

Figures 2 and 3 show typical experimental results (experiment 2 in Table 1). Figure 2 shows how the N₂O absorption signal (as measured in the multipass infrared absorption cell) varied during the measurement cycle after the Nd:YAG laser irradiation at 532 nm was completed. Figure 3 shows how the concentration of O₃ and the number of O(³P_J) atoms generated per laser shot (as measured in the photolysis cell) varied as a function of the laser irradiation time. The experimental procedure employed to obtain the data shown in Figures 2 and 3 is discussed below.

Before the experiment was started, both cells were pumped out, and the transmitted light intensity (I_0) at 253.7 nm was measured. About 2 min later, 1.1 Torr of O₃, with some residual

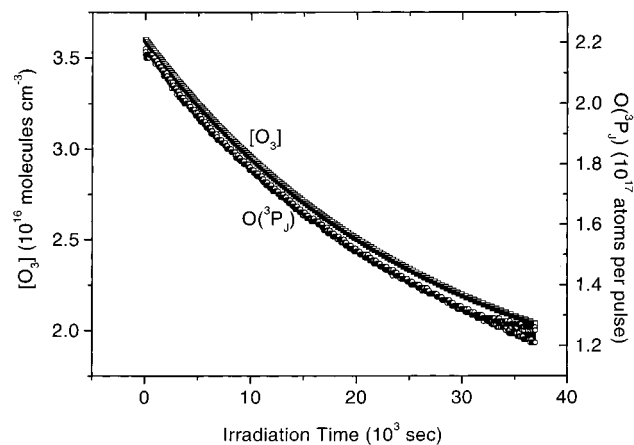


Figure 3. Plot of number of O(³P_J) atoms generated per Nd:YAG laser pulse (empty circles, bottom curve) and [O₃] (empty squares, top curve) versus laser irradiation time in the same experiment shown in Figure 2. Each data point represents an 18-s average.

O₂, was added to the photolysis cell and the transmitted light intensity (I) at 253.7 nm was again measured. The photolysis cell was subsequently filled to a final pressure of 904 Torr by adding synthetic air from its high-pressure tank. For the next 45 min, the O₃/air mixture was allowed to mix thoroughly until the light intensity of the 253.7 nm Hg lamp radiation had stabilized to the same level measured before the addition of synthetic air to the photolysis cell (i.e., I). At this time, the 532 nm irradiation was started and allowed to proceed for 10 h. As depicted in Figure 3, the concentration of O₃ decreased over the irradiation period by a factor of about 1.8. This small drop in the O₃ concentration is the result of the reaction of O(³P_J) with O₃ (even though most of the O₃ photolyzed at 532 nm is regenerated via the recombination reaction $\text{O}(\text{}^3\text{P}_J) + \text{O}_2 + \text{M} \rightarrow \text{O}_3 + \text{M}$). The calculated number of O(³P_J) atoms generated per laser shot is also shown in Figure 3, and as expected, it decreases over the irradiation period since after each laser pulse slightly less O₃ is available to generate O(³P_J) by photolysis. About 1 min after the irradiation period was completed ($t = 1 \text{ min}$ in Figure 2), the multipass cell was filled to 33 Torr with a 0.969 ppmv N₂O standard mixture and its absorption was measured. About 2 min later, the multipass cell was pumped out and the background absorption was obtained from $t = 6 \text{ min}$ to $t = 8 \text{ min}$ by pumping on the cell. At $t = 8 \text{ min}$, the pump-out valve was closed and the valve between the cells was opened so that the reaction products could expand into the infrared cell. The total pressure in the infrared cell was then reduced to about 33 Torr by pumping, and from $t = 9 \text{ min}$ to $t = 10 \text{ min}$ the N₂O content of the reaction products was measured. As observed from Figure 2, only a trace of N₂O, if any, was found to be produced photochemically from this experiment.

Table 1 summarizes the conditions and results from the seven experiments that were performed to study the N₂O yield from the reaction of nascent O₃ with N₂. The experiments can be grouped into three main categories:

- (I) Experiments 1 and 2 were carried out under “normal” conditions.
- (II) Experiments 3 and 4 were “blank” experiments.
- (III) Experiments 5–7 had a known amount of N₂O added to the initial photolysis mixture.

In Table 1, photochemically generated N₂O was taken to be the difference between the number of N₂O molecules detected in a given experiment (category I experiments) and the number

TABLE 1: Summary of Experimental Results from O₃[†] + N₂ Experiments (532 nm Irradiations)

expt no.	initial O ₃ (Torr)	air press. (Torr)	irradiation time (min)	av Nd:YAG		initial N ₂ O (10 ¹² molecules)	N ₂ O detected (10 ¹² molecules)	photolytic		net N ₂ O yield (10 ⁻⁹)
				laser power ^a (mJ/pulse)	N ₂ O detected (10 ¹² molecules)			O(³ P _J) generated (10 ²⁰ atoms)		
1	1.0	904	600	92	0.0	2.8	2.8	2.9	9.8	
2	1.1	904	615	95	0.0	-2.9	-2.9	3.3	-8.9	
3	0.0	900	605	93	0.0	2.8				
4	1.0	905	600 ^b	0	0.0	-2.8				
5	1.0	892	500	95	222	227		2.5		
6	1.0	690	960 ^b	0	127	133				
7	1.0	890	480	95	86	83		2.1		

^a 532 nm. ^b Total time of initial mixture in reaction cell.

of N₂O molecules detected in a “blank” experiment (category II experiments). The net N₂O yield was taken to be the number of photolytically generated N₂O molecules divided by the total number of O(³P_J) atoms produced in the same experiment. The number of O(³P_J) atoms generated per laser shot was calculated as

$$N = (E)(P)(\Phi)(f) \quad (\text{I})$$

where E is the Nd:YAG laser pulse energy, P is the number of photons per millijoule at 532 nm, Φ is the O(³P_J) quantum yield from O₃ photodissociation at 532 nm, and f is the fraction of photons absorbed by the O₃ molecules in the path of the laser beam. The parameter f was calculated as

$$f = 1 - \exp\{-[\text{O}_3](\sigma_{\text{O}_3})_{532 \text{ nm}}(l_1)\} \quad (\text{II})$$

where $(\sigma_{\text{O}_3})_{532 \text{ nm}}$ is the O₃ absorption cross section at 532 nm and l_1 is the laser beam path length (50 cm). The absolute O₃ concentration is derived from the observed 253.7 nm light intensity using Beer's law

$$[\text{O}_3] = \{\ln(I_0/I_t)\}/\{(\sigma_{\text{O}_3})_{253.7 \text{ nm}}(l_2)\} \quad (\text{III})$$

where I_0 is the light level when the reaction cell is empty, I_t is the light level at a time t during the irradiation, $(\sigma_{\text{O}_3})_{253.7 \text{ nm}}$ is the 253.7 nm O₃ absorption cross section, and l_2 is the path length for O₃ detection (i.e., perpendicular to the Nd:YAG laser beam; 5.4 cm).

As mentioned above, category I experiments were carried out under “normal” conditions which were selected to optimize the chances of observing a very small photochemical yield of N₂O (i.e., 900 Torr of total air pressure, 1 Torr of O₃, maximum Nd:YAG laser power at 532 nm, and 10 h irradiation times). In these experiments, the observed N₂O yields were $+9.8 \times 10^{-9}$ and -8.9×10^{-9} , respectively; the average net yield was 4.4×10^{-10} .

In category II experiments, one experiment (experiment 3) was carried out by irradiating 900 Torr of air only and checking the N₂O content of the products after 10 h of irradiation. A second experiment (experiment 4) was carried out by leaving an O₃/air mixture in the reaction cell for 10 h (i.e., laser turned off) and then measuring its N₂O content. The number of N₂O molecules observed in these experiments is not statistically different from the N₂O levels observed in category I experiments. Therefore, the number of N₂O molecules from experiments 3 and 4 were averaged, and that number (essentially zero) was used to compute the number of photolytically generated N₂O molecules in category I experiments.

Category III experiments were designed to verify that the photolysis, transfer, and detection processes could be carried out without *destroying* any photochemically generated N₂O. One experiment (experiment 6) was carried out with the Nd:YAG

laser turned off. In all three cases, the amount of N₂O detected at the end of the experiment was (within the precision of the measurement) equal to the amount of N₂O added to the initial photolysis mixture. The observations from experiments 1–7 suggest that very little, if any, of the N₂O detected was generated photochemically from reaction 4b.

Based on our experimental results, the upper limit quantum yield for production of N₂O from the reaction of nascent O₃ with N₂ is conservatively estimated to be 7×10^{-8} . This value is about a factor of 600 smaller than the value reported by Zipf and Prasad¹² and it is more than an order of magnitude below the threshold for atmospheric importance. In addition, our results suggest that the dominant source of N₂O molecules observed in the preliminary 266 nm experiments is something other than the reaction of nascent O₃ with N₂ (probably the addition of O(¹D₂) to N₂).

In the experiment of Zipf and Prasad,¹² atomic oxygen was produced by the photodissociation of O₂ in ultrapure synthetic air using radiation from a filtered argon flash lamp. All the experiments were performed in a stainless steel photolysis chamber under flow conditions, and N₂O was detected using a gas chromatograph fitted with an electron capture detector. Typically, irradiations lasted for 10–15 min and the N₂O formed in each experiment was cryogenically trapped and concentrated in a small loop before analysis. Zipf and Prasad¹² studied N₂O production over a large pressure range (i.e., 1–1000 Torr), and they employed two reaction vessels of different surface-to-volume ratios in an attempt to discriminate between surface and gas phase reactions. Zipf and Prasad¹² explain the nature of the sources of N₂O in their experiments in terms of two different types of processes (i.e., type I and type II processes). Type I processes, which the authors attribute to surface reactions, appear dominant below 100 Torr, and type II processes, which the authors attribute to gas phase reactions, emerge above 100 Torr. The authors explain that type II processes must be due to gas phase reactions (since surface processes are expected to decrease with increasing pressure), and they suggest that the most likely species responsible for type II production of N₂O is nascent O₃. To obtain the N₂O yield value of 4×10^{-5} from the nascent O₃ + N₂ interaction, Zipf and Prasad¹² were forced to use a complex numerical simulation coupling the chemistries of O, O₃, and nascent O₃ as well as the transport of these species to the reactor walls. By comparison, our study minimizes artifact production of N₂O on various surfaces and, therefore, avoids the use of complex numerical simulations of *likely* interfering reactions as a tool to extract the N₂O yield.

Zipf and Prasad¹² carried out their study motivated by several laboratory experiments suggesting the production, or lack of production, of N₂O from various mixtures of N₂, O₂, and O₃.^{45–50} Nevertheless, Zipf and Prasad¹² have suggested in their analysis that the small N₂O yield obtained in most of these other literature studies could be explained by a loss process destroying

TABLE 2: Summary of Kinetic Data for the Reaction O(¹D₂) + N₂ + M → N₂O + M

<i>T</i> (K)	air press. (Torr) ^a	N ₂ O yield (10 ⁻⁶)	O(¹ D ₂) generated (10 ²⁰ atoms)	no. of expts ^c	<i>k</i> ₆ ^d (10 ⁻³⁶ cm ⁶ molecule ⁻² s ⁻¹)
324	401–805	0.9–1.7	0.3–0.6	4	2.62 ± 0.28
295	192–793 ^b	0.5–1.9	0.3–1.1	6	2.68 ± 0.43
270	193–802	0.4–2.1	0.4–2.2	7	3.13 ± 0.46
243	178–778	0.5–2.4	0.9–3.2	4	3.56 ± 0.51
220	152–760	0.4–2.3	0.5–1.2	4	3.48 ± 0.65

^a Typical initial [O₃] ranged from 9.5 × 10¹⁵ to 9.8 × 10¹⁵ molecules cm⁻³ unless otherwise noted. ^b Two experiments, at 198 and 793 Torr, were performed with an initial [O₃] of 4.5 × 10¹⁵ molecules cm⁻³. ^c Experiment ≡ determination of a single N₂O yield at a given air pressure. ^d Individual rate coefficients shown in the table have been corrected for the effect of reaction 2. Uncertainties are 2σ and represent precision only.

any N₂O formed via reaction 4b when O₃ is present initially in the reaction cell. However, category III experiments from our study tested this hypothesis, and they conclusively rule out an efficient N₂O loss process under our experimental conditions.

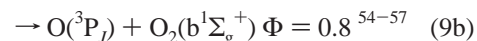
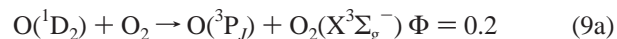
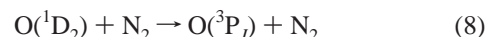
Another potential point of concern is the possibility that ground state O₃ could have rapidly deactivated vibrationally excited O₃ and, thus, suppressed N₂O formation. It is interesting to note that our experiments were designed to greatly increase the N₂-to-O₃ ratio by using only 1 Torr of O₃ in 900 Torr of air (compared to 5–100 Torr of O₃ in typical mixtures employed in previous experiments). In addition, the N₂-to-O₃ ratio was even smaller in the preliminary 266 nm experiments (where only 0.1–0.3 Torr of O₃ was initially present in the reaction cell). Nonetheless, the O₃:air ratio employed in our experiments is several orders of magnitude larger than the O₃:air ratio in the atmosphere. Even though there is no direct information in the literature on the average energy removed from internally excited O₃ per collision with diatomics and triatomics, information is available on the average energy removed per collision from internally excited SO₂, CS₂, and NO₂ by several monatomic, diatomic, and triatomic species.^{51–53} Focusing our attention on internally excited NO₂, which is the most thoroughly studied molecule of the three, it has been observed that at high internal excitation energies the ratio of the energy removed by a collision with N₂ or O₂ is only about a factor of 5 smaller than the energy removed per collision by triatomics such as CO₂, N₂O, and NO₂.⁵² Furthermore, the available evidence suggests that there is no significant enhancement in the average energy removed per collision when the collider and the excited species are chemically identical, i.e., the average energy removed in NO₂[†]–NO₂ collisions is about the same as the average energy removed in collisions of NO₂[†] with other triatomic molecules. Assuming that O₃ behaves similarly to the molecules studied by Hartland et al.^{51,52} and Chimbayo et al.,⁵³ it seems highly unlikely that O₃ could have competed with N₂ + O₂ at deactivating vibrationally excited O₃ under our experimental conditions.

3.3. Temperature-Dependent 266 nm Irradiation Experiments. *3.3.1. Kinetic Results.* Under the assumption that all N₂O observed in the 266 nm photolysis experiments is produced via reaction 6, the N₂O yield data can be employed to obtain values for *k*₆(*T*). Rate coefficients were evaluated at five different temperatures ranging from 220 to 324 K, and the results are summarized in Table 2. The net N₂O yield was taken to be the number of photolytically generated N₂O molecules divided by the number of O(¹D₂) atoms produced in the same experiment. Since the “blank” runs yielded negligible N₂O in the preliminary experiments, photolytically generated N₂O was simply taken

to be the number of N₂O molecules detected in a given 266 nm irradiation. Note that the 295 K rate coefficient measured in this set of experiments is within 5% of the value determined in the preliminary experiments.

Unlike the 532 nm experiments, readily measurable levels of N₂O were observed at all pressures and temperatures investigated. Irradiation times ranged from 10 to 110 min and, in most cases, irradiations were stopped when approximately 50 ppbv N₂O was expected to have been generated in the photolysis cell (about 30 ppbv in those experiments performed at the lowest pressures and highest temperatures). As observed from Table 2, the yield of N₂O was obtained at four or more different pressures per temperature investigated. The number of O(¹D₂) atoms generated per laser shot was calculated as in eq I with the difference that Φ = 0.88³⁶ and *P* is the number of photons per millijoule at 266 nm. The fraction of photons absorbed by the O₃ molecules in the photolysis cell was also computed as in eq II, but in this case, the O₃ absorption cross section at 266 nm was used instead of the O₃ absorption cross section at 532 nm. As mentioned in the Experimental Section, a direct measurement of the fraction of laser photons absorbed by the O₃ molecules in the reaction cell was also performed. If *I*₀ is taken to be the number of transmitted 266 nm photons when the reaction cell is empty and *I* is taken to be the number of transmitted photons at any time during the 266 nm irradiation, the difference (*I*₀ – *I*) directly gives the number of O(¹D₂) atoms produced. On average, the two determinations of the number of O(¹D₂) atoms generated over the course of a given irradiation agreed to within ±4%.

Rate coefficients for reaction 6 were computed from the net N₂O yields. Figure 4 shows two sample plots of the pressure dependence of the net N₂O yields obtained at *T* = 220 and 295 K. At all five temperatures investigated, the plots were linear, which is consistent with N₂O production via a termolecular process that occurs in competition with a bimolecular process, i.e., deactivation of O(¹D₂) to O(³P_{*J*}) by N₂ and O₂:



As a result, the net N₂O yield is the ratio of the rate of reaction 6 divided by the sum of the rates of reactions 6, 8, and 9. Since *k*₆[N₂][M] ≪ *k*₈[N₂] + *k*₉[O₂], it then follows that the association rate coefficient for reaction 6 at each temperature can be computed from the following expression:

$$k_6 = \Phi(P)\{k_8[\text{N}_2] + k_9[\text{O}_2]\}/[\text{N}_2][\text{M}] \quad (\text{IV})$$

where Φ(*P*) is the pressure-dependent N₂O yield and [M] is the total gas concentration. Although *x*-intercepts in Figure 4 do vary systematically with temperature, they are always within the reported 2σ uncertainty (precision only) of zero.

The temperature-dependent rate coefficients for reaction 9 were obtained from the current NASA panel recommendation.⁵⁸ On the other hand, the rate coefficients for reaction 8 were derived from expression V:

$$k_8(T) = 2.1 \times 10^{-11} \exp(115/T) \text{ cm}^3 \text{ molecule}^{-1} \text{ s}^{-1} \quad (\text{V})$$

Expression V is based on recent results from three laboratories which suggest that *k*₈(*T*) is somewhat faster than previously thought.⁵⁹ It is interesting to note that using the 2000 NASA

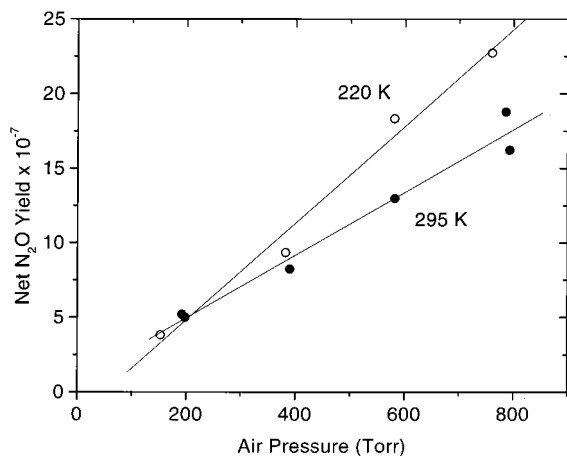


Figure 4. Plots of net N₂O yield versus air pressure for data obtained in the study of reaction 6 at $T = 220$ and 295 K. Solid lines are obtained from least-squares analyses. Their slopes give the following values in units of 10^{-9} Torr⁻¹: 3.24 ± 0.60 at 220 K and 2.10 ± 0.34 at 295 K. Their intercepts give the following values (where uncertainties are 2σ and represent precision only): $(-1.65 \pm 3.10) \times 10^{-7}$ at 220 K and $(0.76 \pm 1.88) \times 10^{-7}$ at 295 K.

panel recommended expression for $k_8(T)$ in eq IV to compute $k_6(T)$ would lead to rate coefficients about 12% smaller than those obtained using expression V. These changes are well within our reported uncertainties in $k_6(T)$ (see error analysis discussion below).

An Arrhenius plot for reaction 6 is shown in Figure 5. The temperature dependence of reaction 6 is characterized by a small negative activation energy. A linear least-squares analysis of the $\ln k_6$ vs $1/T$ data gives the following expression:

$$k_6(T) = (1.3 \pm 0.5) \times 10^{-36} \times \exp\{(230 \pm 110)/T\} \text{ cm}^6 \text{ molecule}^{-2} \text{ s}^{-1} \quad (\text{VI})$$

Uncertainties in the above expression are 2σ and represent precision only. These uncertainties refer to the Arrhenius parameters only. Error estimates for individual rate coefficients are derived below.

The NASA panel for chemical kinetics and photochemistry data evaluation⁵⁸ typically approximates the temperature dependence of rate coefficients for association reactions in their low-pressure regime with an expression of the form

$$k_0(T) = k_0(300 \text{ K})(T/300)^{-n} \quad (\text{VII})$$

Fitting our measured values to eq VII gives the following expression:

$$k_{6,0}(T) = (2.8 \pm 0.1) \times 10^{-36} (T/300)^{-(0.88 \pm 0.36)} \times \text{cm}^6 \text{ molecule}^{-2} \text{ s}^{-1} \quad (\text{VIII})$$

Once again, the stated uncertainties refer to the fit parameters only (i.e., they represent 2σ precision). It is worth noting that this is the first time that a temperature-dependent kinetics study of reaction 6 has been reported.

At each temperature and pressure investigated, it becomes necessary to consider the effect of reaction 2 on the observed net N₂O yields. Thus, to perform the appropriate corrections to our kinetic data, we decided to simulate our experiments using ACUCHEM, a numerical integration routine written at the National Institute of Standards and Technology. Table 3 shows the chemical mechanism used in our simulations including the

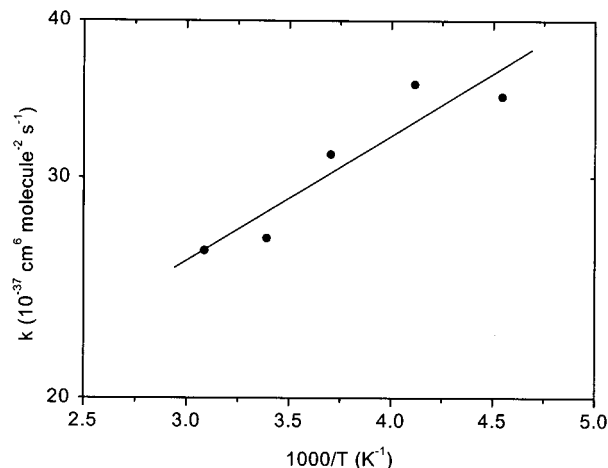


Figure 5. Arrhenius plot for reaction 6. The solid line is obtained from a least-squares analysis which weights each data point equally; it represents the Arrhenius expression given in the text. Individual rate coefficients have been corrected for the effect of reaction 2.

TABLE 3: Reaction Mechanism Used To Simulate the 266 nm Kinetics Experiments

reaction	k^a
$\text{O}_3 + h\nu \rightarrow \text{O}(^1\text{D}) + \text{O}_2(^1\Delta)$	$0.15^{b,c}$
$\rightarrow \text{O}(^3\text{P}) + \text{O}_2$	$0.02^{b,c}$
$\text{O}(^1\text{D}) + \text{O}_2 \rightarrow \text{O}(^3\text{P}) + \text{O}_2$	8.0×10^{-12}
$\rightarrow \text{O}(^3\text{P}) + \text{O}_2(^1\Sigma)$	3.2×10^{-11}
$\text{O}(^1\text{D}) + \text{O}_3 \rightarrow \text{O}_2 + \text{O}_2$	1.2×10^{-10}
$\rightarrow 2\text{O}(^3\text{P}) + \text{O}_2$	1.2×10^{-10}
$\text{O}(^1\text{D}) + \text{N}_2\text{O} \rightarrow \text{N}_2 + \text{O}_2$	4.9×10^{-11}
$\rightarrow \text{NO} + \text{NO}$	6.7×10^{-11}
$\text{O}(^1\text{D}) + \text{N}_2 \rightarrow \text{O}(^3\text{P}) + \text{N}_2$	3.0×10^{-11}
$\text{O}(^1\text{D}) + \text{N}_2 + \text{M} \rightarrow \text{N}_2\text{O}$	2.6×10^{-36d}
$\text{O}_2(^1\Delta) + \text{O}_3 \rightarrow \text{O}(^3\text{P}) + 2\text{O}_2$	3.8×10^{-15}
$\text{O}_2(^1\Delta) + \text{O}_2 \rightarrow \text{products}$	1.7×10^{-18}
$\text{O}_2(^1\Delta) + \text{N}_2 \rightarrow \text{products}$	1.0×10^{-20}
$\text{O}_2(^1\Delta) \rightarrow \text{O}_2$	$0-20^b$
$\text{O}_2(^1\Delta) + \text{O} \rightarrow \text{products}$	2.0×10^{-16}
$\text{O}_2(^1\Sigma) + \text{N}_2 \rightarrow \text{products}$	2.1×10^{-15}
$\text{O}_2(^1\Sigma) + \text{O}_2 \rightarrow \text{products}$	3.9×10^{-17}
$\text{O}_2(^1\Sigma) + \text{O}_3 \rightarrow \text{O}(^3\text{P}) + 2\text{O}_2$	1.5×10^{-11}
$\rightarrow \text{products}$	6.6×10^{-12}
$\text{O}_2(^1\Sigma) + \text{O} \rightarrow \text{products}$	8.0×10^{-14}
$\text{O} + \text{O}_2 + \text{M} \rightarrow \text{O}_3$	6.2×10^{-34d}
$\text{O} + \text{O}_3 \rightarrow 2\text{O}_2$	8.0×10^{-15}

^a Rate coefficients used to simulate the room-temperature experiments. Units are $\text{cm}^3 \text{ molecule}^{-1} \text{ s}^{-1}$ unless otherwise noted. Temperature-dependent rate coefficients for each reaction in the simulation were primarily obtained from the expressions recommended by the 2000 NASA panel.⁵⁸ Exceptions were the temperature-dependent rate coefficients for reaction 8, where expression V was employed instead (see discussion in text), and the temperature-dependent rate coefficients for reaction 6, where the rate coefficients derived from this study were used instead. The third-order rate coefficient entered for reaction 6 was obtained after running the model at each pressure studied at 295 K and correcting the individual N₂O yields at each pressure investigated (i.e., the calculation of the final temperature-dependent rate coefficients for reaction 6 shown in Table 2 was an iterative process). ^b Units are s^{-1} . ^c Typical first-order O₃ decay rate used to model the O₃ concentration. The O₃ decay rate shown in the table was used to model one experiment carried out under the following conditions: $P = 192$ Torr; $T = 295$ K; $[\text{O}_3]_0 = 9.8 \times 10^{15} \text{ molecules cm}^{-3}$. ^d Units are $\text{cm}^6 \text{ molecule}^{-2} \text{ s}^{-1}$.

rate coefficients employed to simulate the room-temperature experiments.

Initially, we attempted to simulate the total number of N₂O molecules produced and destroyed in each experiment by matching the ACUCHEM-simulated O₃ profile to the experimentally observed O₃ profile (ACUCHEM most conveniently

simulates the photolysis of O₃ with a first-order decay rate). Trial-and-error inputs of different first-order O₃ decay rates were made until a suitable match between both profiles was obtained. However, it was found that, in every case, the model overestimated the total number of O(¹D₂) atoms generated during the irradiation period (typically by factors of 1.4–2.0), and thus it overestimated the total number of N₂O molecules detected (by approximately the same factor). This motivated us to modify our modeling approach and change the model input of the first-order O₃ decay rate (once again by trial and error) to one that would lead to a close match between the calculated and simulated total number of O(¹D₂) atoms generated in each experiment. With this new procedure, good matches were readily obtained and the total number of N₂O molecules generated in each experiment was properly simulated (within the precision of the N₂O detection measurement). Nonetheless, this second approach required inputting a smaller value for the O₃ first-order decay rate than the one used when attempting to match the O₃ profiles. A combination of two possible factors can perhaps explain the mismatch between O₃ profiles. The first one is the fact that we are unable to model properly the experimental O₃ profile with ACUCHEM because we assumed a first-order photolysis rate when, in reality, the effective first-order O₃ decay rate changed as a function of irradiation time (due to optical thickness effects). Alternatively, the disagreement in the O₃ profiles could be suggestive of the possible presence of one or more additional O₃ loss process(es) not considered in our chemical mechanism (see Table 3). It is interesting to note that an additional unidentified O₃ loss process is not present when the laser is turned off or when 532 nm radiation is used instead of 266 nm irradiation (concluded after a similar ACUCHEM simulation of the 532 nm irradiation experiments). Even though the exact nature of the additional O₃ loss process (if any) is not clear at this time, it is important to point out that its possible presence would not affect the value of our net N₂O yields, or our calculated rate coefficients for reaction 6. This is the case because the number of O(¹D₂) atoms generated per laser pulse was calculated from the *measured* O₃ profile and not from the simulated O₃ profile. Moreover, it seems unlikely that a process other than photolysis would lead to the production of O(¹D₂) atoms.

Based on the 266 nm ACUCHEM simulations (using the second approach described above), it was calculated that, on average, about 10% of the total number of N₂O molecules produced photolytically were destroyed by reactions 2a and 2b over the course of each irradiation experiment (i.e., the percentage of N₂O destroyed actually ranged from 4% to 23% depending on conditions and irradiation time). Changes to individual net N₂O yields led to changes of typically less than 10% in $k_6(T)$. Therefore, even if the ACUCHEM simulations were somewhat uncertain, the rate coefficients would not change much.

One potential complication in the 266 nm photolysis experiments concerns the long-lived species O₂(a¹Δ_g), which is generated directly from O₃ photolysis and also from the O(¹D₂) + O₂ interaction via the intermediate O₂(b¹Σ_g⁺) (see Table 3). O₂(a¹Δ_g) is sufficiently stable that it is not expected to completely decay away during the 0.1 s between laser flashes. Hence it is necessary to consider the possibility that 266 nm photolysis of O₂(a¹Δ_g) could be an additional source of O(¹D₂) that must be accounted for in the data analysis. This possibility can, however, be ruled out on energetic grounds since, based on the best available thermochemical information,⁵⁸ the only energetically allowed photolysis channel for O₂(a¹Δ_g) + *hν*-

(266 nm) is production of two O(³P_J). Since the only allowed photolysis channel is spin-forbidden, one would expect the O₂-(a¹Δ_g) absorption cross section at 266 nm to be very small. To our knowledge, no measurements of O₂(a¹Δ_g) absorption cross sections have been reported at wavelengths longer than 200 nm. However, theoretical calculations of long-wavelength absorption cross sections have been reported⁶⁰ that confirm the expected very small absorption cross section, i.e., $\sigma(266 \text{ nm}) \approx 4 \times 10^{-24} \text{ cm}^2 \text{ molecule}^{-1}$.

3.3.2. Estimated Accuracy of Reported Rate Coefficients. The three major contributors to the overall accuracy of the rate coefficients in this temperature-dependent kinetic study of the addition of O(¹D₂) to N₂ are the precision of the net N₂O yields, the accuracy of the total number of O(¹D₂) atoms generated per laser pulse, and the uncertainty in the literature values for reactions 8 and 9. These sources of error are discussed below.

The accuracy of the total number of O(¹D₂) atoms generated per laser pulse is a function of the uncertainty in the following factors: the measurement of the total number of incoming laser photons, the measurement of the fraction of photons absorbed by the O₃ molecules in the reaction cell, and the literature value for the quantum yield for production of O(¹D₂) in the photolysis of O₃ at 266 nm. We estimate that the accuracy of our measurement of the total number of incoming laser photons is ±5%. The quantum yield for production of O(¹D₂) is known to ±3%.³⁶ The accuracy of the fraction of photons absorbed by the O₃ molecules in the reaction cell is itself a function of the accuracy in the measurement of the O₃ concentration and the uncertainty in the literature value for the O₃ absorption cross section at 266 nm. We estimate that our measurement of the O₃ concentration has a ±3% uncertainty (which itself includes a ±1% error in both *I* and *I*₀, and a ±2% error in the O₃ absorption cross section at 253.7 nm⁵⁸). On the other hand, the O₃ absorption cross section at 266 nm is known within ±3%.⁵⁸ Therefore, the estimated accuracy of the fraction of photons absorbed by O₃ is ±4%. Combining all the above factors together, the error in the total number of O(¹D₂) atoms generated in each irradiation is estimated to be about ±7%.

Examination of Table 2 shows that on average the precision of the net N₂O yields is ±15%. Conservatively estimating that the ACUCHEM simulations lead to an additional ±5% error in the net N₂O yields, we estimate that the accuracy of the total number of N₂O molecules measured in our study is ±16%. Combining the error in the determination of the total number of N₂O molecules with that of the total number of O(¹D₂) atoms, we obtain a preliminary overall error in our reported rate coefficients of ±17%. As indicated by eq IV, the temperature-dependent rate coefficients for reaction 6 depend, in our analysis, on the temperature-dependent rate coefficients for reactions 8 and 9. Both of those rate coefficients are known to ±20% at room temperature and to ±35% at 220 K.⁵⁸ Combining the accuracy in our reported rate coefficients (i.e., ±17%) with the uncertainty in the literature values for reactions 8 and 9 leads to an overall accuracy of ±27% in our reported room-temperature rate coefficient and to an overall accuracy of ±39% in our 220 K rate coefficient. The following format is widely used to express uncertainties in rate parameters that are used in modeling atmospheric chemistry:⁵⁸

$$f(T) = f(298 \text{ K}) \exp\{(\Delta E_a/R)(T^{-1} - 298^{-1})\} \quad (\text{IX})$$

Applying expression IX to our results leads to the following estimated parameters: $f(298 \text{ K}) = 1.27$ and $(\Delta E_a/R) = 75$.

3.3.3. Comparison of Reported Rate Coefficients with Literature Values. As mentioned above, there are three literature

TABLE 4: Summary of Literature Values for the $O(^1D_2) + N_2 + M$ Rate Coefficient

reference	N_2O detection technique	P (atm)	$k_6(298\text{ K})$ ($10^{-36}\text{ cm}^6\text{ molecule}^{-2}\text{ s}^{-1}$)	E_a (kJ mol^{-1})
Gaedtke et al. (1972) ³¹	GC ^a	1–200	2.8 ± 1.4^b	
Kajimoto and Cvetanovic (1976) ³²	GC	20–120	0.35 ± 0.30^c	
Maric and Burrows (1992) ³³	GC	1	0.88 ± 0.33	
this work	TDLAS ^d	0.1–1.2	2.8 ± 0.8	-1.9 ± 0.9

^a Gas chromatography. ^b Upward revision appears necessary (see text). ^c Error bar estimated by NASA panel.⁵⁸ ^d Tunable diode laser absorption spectroscopy.

reports of the room-temperature rate coefficient for reaction 6, i.e., Gaedtke et al.,³¹ Kajimoto and Cvetanovic³² (which is the basis of the current NASA panel recommendation⁵⁸), and Maric and Burrows.³³ Each one of them is discussed below. Table 4 summarizes the literature values for k_6 .

The first reported study of reaction 6 was performed by Gaedtke et al.³¹ These investigators introduced 20 Torr of O_2 , 0.2 Torr of O_3 , and 1–200 atm of N_2 buffer gas into a steel reaction tube. O_3 photolysis was carried out with a 200 W Xe–Hg lamp and irradiation times lasted between 1 and 20 min. After the irradiation period, N_2O was collected in a trap and analyzed by gas chromatography. Both the quantum yield for O_3 photolysis at 260 nm and the number of N_2O molecules measured per O_3 molecule destroyed (defined by the authors as the “ N_2O yield”) were measured as functions of N_2 pressure. Gaedtke et al.³¹ observed that the N_2O yield increased with increasing pressure up to a value close to unity at very high pressure. To obtain a value for the room-temperature rate coefficient for reaction 6, the authors approximated their observed N_2O yield by a ratio of the rate of reaction 6 divided by the sum of the rates of reaction 6 and twice the rate of reaction 10:



using a value of $2.5 \times 10^{-10}\text{ cm}^3\text{ molecule}^{-1}\text{ s}^{-1}$ for k_{10} . As a result, Gaedtke et al.³¹ obtained a room-temperature rate coefficient for reaction 6 of $(2.8 \pm 1.4) \times 10^{-36}\text{ cm}^6\text{ molecule}^{-2}\text{ s}^{-1}$. Interestingly, this value is virtually identical to our room-temperature rate coefficient derived from expression VI! Nonetheless, it is our opinion that the expression that Gaedtke et al.³¹ used to derive their third-order room-temperature rate coefficient should be modified. First, it is currently believed that the rate coefficient for reaction 10 is $1.2 \times 10^{-10}\text{ cm}^3\text{ molecule}^{-1}\text{ s}^{-1}$.⁵⁸ In addition, it appears that the reaction of $O(^3P_J)$ atoms with O_3



contributed as an important ozone loss process under the experimental conditions employed by Gaedtke et al.³¹ Quantitative reanalysis of Gaedtke et al.’s data is not possible because, at the high pressures employed in their study, a complex energy transfer scheme may be operative³² (see below) that results in a nonlinear dependence of N_2O yield on pressure.

In the study of Kajimoto and Cvetanovic,³² excited oxygen atoms were generated by photolyzing O_3 at wavelengths between 220 and 280 nm using filtered radiation from a 500 W Hanovia medium-pressure Hg lamp. Experiments were performed in a quartz reaction cell containing typically 10 Torr of O_3 , 100 Torr of O_2 , and 20–120 atm of N_2 . After a period of irradiation ranging from 13 to 48 h, the resulting N_2O was cryogenically trapped and measured by gas chromatography. Kajimoto and Cvetanovic³² observed that the N_2O quantum yield increased

as a function of the square of the nitrogen pressure. Extrapolation of their results to 1 atm leads to a quantum yield for N_2O production of 3.1×10^{-7} , which translates into a room-temperature rate coefficient of $3.5 \times 10^{-37}\text{ cm}^6\text{ molecule}^{-2}\text{ s}^{-1}$ (i.e., about a factor of 7.5 slower than the one derived from this study).

Like Gaedtke et al.,³¹ Kajimoto and Cvetanovic³² were forced to study reaction 6 at very high N_2 pressures (20–120 atm) due to their relatively poor N_2O detection sensitivity. As a result, Kajimoto and Cvetanovic³² performed a long extrapolation in order to derive the N_2O yield at a pressure of 1 atm. The disadvantage of such an approach is that a small systematic error in the N_2O yield measured at high pressures can result in a large error in the extrapolated N_2O yield at 1 atm (even though their N_2O yield data appear to have excellent precision). The better N_2O detection sensitivity in our study permitted kinetic measurements at lower, more realistic atmospheric pressures. It is also interesting to note that Kajimoto and Cvetanovic³² observed a quadratic dependence of the N_2O quantum yield on pressure in the high-pressure regime, whereas our lower pressure results show a linear dependence of the N_2O yield on pressure.

As discussed by Kajimoto and Cvetanovic,³² a nonlinear dependence of N_2O yield on pressure can be rationalized if it is assumed that multiple collisions with the bath gas are required to deactivate newly formed N_2O to an energy sufficiently low that crossing to a triplet surface (and subsequent rapid dissociation to $O(^3P_J) + N_2$) cannot occur. When $O(^1D_2)$ interacts with N_2 , it is thought that some energy is rapidly shunted into N_2 vibration, yielding an energized complex with a rather long lifetime (estimated to be 1–10 ps; i.e., hundreds of vibrational periods) toward dissociation back to reactants.^{61–63} Hence, the lifetime of energized N_2O is limited by the rate of crossing to the triplet surface which, in the absence of collisions, occurs with essentially unit probability in competition with dissociation back to reactants.^{61,62} For our experimental conditions, where the mean time between collisions ranged from 100 to 1000 ps, it seems reasonable that most N_2O is generated when a single collision with the bath gas deactivates the energized complex to an internal energy where crossing to the triplet surface cannot occur (i.e., the probability of an energized complex experiencing multiple collisions during its lifetime is very small). On the other hand, a multiple collision mechanism may have been operative under the high-pressure conditions employed by Kajimoto and Cvetanovic.³²

In the study performed by Maric and Burrows,³³ a mixture of 3350 ppm O_3 in synthetic air at 1 atm pressure was irradiated with a filtered ($\lambda \geq 254\text{ nm}$) low-pressure mercury lamp. The reaction cell was made of Pyrex and it was equipped with Suprasil windows. The concentration of O_3 was monitored photometrically at 311.6 nm using radiation from a D_2 lamp. The mixing ratio of N_2O was determined by cryogenically trapping the reaction products and transferring a 2 mL sample (with a gastight syringe) to a gas chromatograph fitted with an electron capture detector. Maric and Burrows³³ calculated the

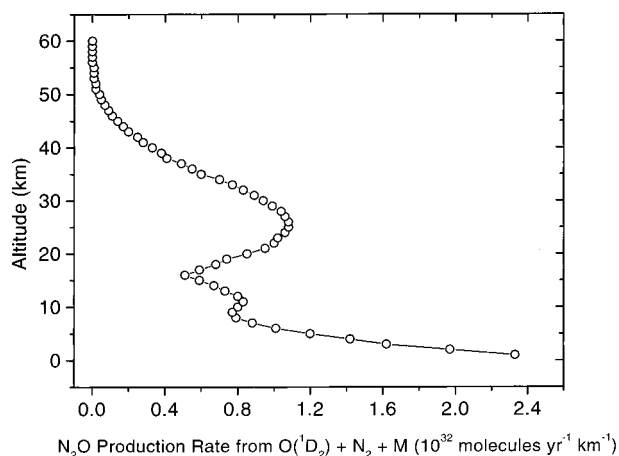


Figure 6. Altitude dependence of annual N₂O production rate from processes initiated by absorption of an ultraviolet photon by O₃. Yields of N₂O reported in this study are used to evaluate the production rates. Each data point represents a globally averaged integration over the next 1 km.

room-temperature rate coefficient for reaction 6 from the measured rate of formation of N₂O, the measured decay rate of O₃, and the mean O₃ concentration during the irradiation period. Their value of $(8.8 \pm 3.3) \times 10^{-37} \text{ cm}^6 \text{ molecule}^{-2} \text{ s}^{-1}$ is a factor of 2.5 faster than the value derived by Kajimoto and Cvetanovic,³² although the values agree to within combined error limits; their value is approximately a factor of 3 lower than the value reported in this study. The study of Maric and Burrows³³ employed total pressures similar to those used in our study. Unfortunately, it is difficult to comment on the accuracy of the data analysis and determination of N₂O quantum yields in the study of Maric and Burrows³³ due to the lack of detail given in their paper.

3.3.4. Implications for Atmospheric Chemistry. To assess the potential importance of reaction 6 as an atmospheric source of N₂O, a total yearly N₂O production rate was calculated using the kinetic data obtained in our study of reaction 6. O₃ concentrations above 100 mbar were obtained from the middle atmospheric model of Wang et al.⁶⁴ Below 100 mbar, O₃ concentrations were obtained from observed O₃ distributions in the troposphere.⁶⁵ O₃ photolysis rates were computed from the chemical model developed by Ramarosan et al.⁶⁶ together with updated O(¹D₂) quantum yield data from Sander et al.⁵⁸ The total number of N₂O molecules generated per year in the troposphere and the stratosphere was calculated to be 3.8×10^{33} . Figure 6 shows the altitude dependence of the annual N₂O production rate from reaction 6, where each data point represents a globally averaged integration over the next 1 km. The troposphere accounts for only about one-third of the total N₂O production rate, while the stratosphere accounts for about two-thirds of the total N₂O production rate. The most recent study of the atmospheric N₂O budget by Kroeze et al.⁸ suggests that the input flux of N₂O into the atmosphere is approximately 3.9×10^{35} molecules per year, even though recent estimates range from 2.1×10^{35} to 3.9×10^{35} molecules per year.^{3,7-9} Based on the above analysis, and considering the uncertainty in the global flux of N₂O into the atmosphere, reaction 6 represents a source that is about $1.4 \pm 0.4\%$ of the estimated total N₂O source strength.

An approximate 1.4% contribution from reaction 6 to the global yearly N₂O source strength, although seemingly small, may have important implications for the observed isotopic composition of N₂O in the atmosphere. As mentioned in the

Introduction, since O(¹D₂) is generated from the photolysis of O₃, and since O₃ has been observed to be isotopically mass-independently enriched in the atmosphere (with an extraordinarily large ¹⁷O excess of $\Delta^{17}\text{O} \approx 30\%$),²⁶⁻²⁸ reaction 6 could contribute to the observed mass-independent enrichment of N₂O. To explain the entire ¹⁷O excess of $\Delta^{17}\text{O} \approx 1\%$ in atmospheric N₂O,^{13,14,30} about 3% of the total N₂O source strength must originate from an N₂O source stemming from O₃. Since our results suggest that reaction 6 constitutes about 1.4% of the currently estimated total N₂O source strength, the contribution of reaction 6 to the N₂O budget is of the right magnitude to account for a significant fraction of the oxygen mass-independent enrichment observed in atmospheric N₂O. As noted above, about two-thirds of the total atmospheric N₂O production from reaction 6 takes place in the stratosphere. This finding is consistent with the observation by Cliff et al.¹⁴ that stratospheric N₂O displays larger oxygen mass-independent enrichments than tropospheric N₂O. Although an additional N₂O source may be necessary to explain the observed ¹⁷O excess of $\Delta^{17}\text{O} \approx 1\%$, this is the first time that a mechanism that generates N₂O photochemically in the atmosphere has been reported that may explain the altitude dependence of the N₂O isotopic signature. Even though the mechanism proposed by Rockmann et al.³⁰ (i.e., transfer of mass independently enriched oxygen from O₃ to NO₂, followed by a second transfer to N₂O via the reaction $\text{NO}_2 + \text{NH}_2 \rightarrow \text{N}_2\text{O} + \text{H}_2\text{O}$) can partially explain the N₂O mass-independent fractionation in the troposphere, the coupling of the proposed mechanism to the ammonia cycle means that it cannot account for the increase in mass-independent oxygen enrichment in stratospheric N₂O. It does appear, however, that reaction 6 together with the mechanism proposed by Rockmann et al.³⁰ could potentially fully explain the mass-independent oxygen isotope fractionation of tropospheric and stratospheric N₂O.

3.3.5 Alternate Interpretation of the 266 nm Photolysis Experiments. In a recent conference presentation,⁶⁷ Prasad has suggested that the N₂O observed in our 266 nm photolysis experiments may not result from the O(¹D₂) + N₂ association reaction, but rather from the reaction of undissociated electronically excited O₃ (lifetime ~ 10 fs) with N₂. To justify his somewhat more exotic interpretation of our results, Prasad cites the faster value for k_6 obtained from our data (compared to the value reported by Kajimoto and Cvetanovic³²) and the linear dependence of the N₂O yield on pressure observed in our experiment (compared to the quadratic dependence observed in the higher pressure study of Kajimoto and Cvetanovic³²). At this time there does not appear to be any theoretical or experimental information available to definitively rule out Prasad's suggestion. On the other hand, there is no experimental or fundamental theoretical information available to support Prasad's suggestion, either. Pending further experimental and/or theoretical research on this issue, we consider O(¹D₂) + N₂ association to be the probable source of the N₂O observed in our 266 nm photolysis experiments.

It is worth noting that the atmospheric implications discussed in section 3.3.4 are essentially independent of whether N₂O is produced from O(¹D₂) + N₂ or from electronically excited O₃ + N₂. The model calculation of annual N₂O production would be identical in the two cases as long as it is assumed that only the excited O₃ electronic state that dissociates to singlet products can interact with N₂ to produce N₂O. Similarly, since O₃ provides the O atom to N₂O in both cases, the potential contribution to mass-independent isotope effects is also independent of which of the two possible pathways is operative.

Acknowledgment. The experimental component of this research was supported by the National Aeronautics and Space Administration through Grant NAG5-8931 and by the National Science Foundation through Grant ATM-99-10912, while the modeling component was supported by the National Aeronautics and Space Administration through Grant NAG1-2202. We thank Dr. Robert E. Stickel for technical assistance with the TDLAS system. We also thank Professor John Barker for helpful discussions concerning energy transfer from highly vibrationally excited molecules and Dr. Tom Slanger for helpful discussions concerning $O_2(a^1\Delta_g)$ photochemistry. Finally, we thank Dr. Sheo Prasad for communicating his most recent results to us prior to publication.

References and Notes

- Minschwaner, K.; Salawitch, R. J.; McElroy, M. B. *J. Geophys. Res.* **1993**, *98*, 10543.
- Dickinson, R. E.; Cicerone, R. J. *Nature* **1986**, *319*, 109.
- Prather, M.; Ehhalt, D.; Dentener, F.; Derwent, R.; Dlugokencky, E.; Holland, E.; Isaksen, I.; Katima, J.; Kirchoff, V.; Matson, P.; Midgley, P.; Wang, M. *Climate Change 2001: The Scientific Basis, Chapter 4*; Contribution of working group I to the third assessment report of the Intergovernmental Panel on Climate Change; Houghton, J. T., Ding, Y., Griggs, D. J., Noguer, M., van der Linden, P. J., Dai, X., Maskell, K., Johnson, C. A., Eds.; Cambridge University Press: Cambridge, UK, 2001.
- Cantrell, C. A.; Shetter, R. E.; Calvert, J. G. *J. Geophys. Res.* **1994**, *99*, 3739.
- García, R. R.; Solomon, S. *J. Geophys. Res.* **1994**, *99*, 12937.
- World Meteorological Organization (WMO). *Scientific Assessment of Ozone Depletion: 1998, Report No. 44*; Global Ozone Research and Monitoring Project: Geneva, Switzerland, 1999, and references therein.
- Mosier, A.; Kroeze, C. *IGBP Global Change Newslett.* **1998**, June (No. 34), 8–13.
- Kroeze, C.; Mosier, A.; Bouwman, L. *Global Biogeochem. Cycles* **1999**, *13*, 1.
- Olivier, J. G. J.; Bouwman, A. F.; van der Hoek, K. W.; Berdowski, J. J. M. *Environ. Pollut.* **1998**, *102*, 135.
- Zellner, R.; Hartmann, D.; Rosner, I. *Ber. Bunsen-Ges. Phys. Chem.* **1992**, *96*, 385.
- Delmdahl, R. F.; Gericke, K.-H. *Chem. Phys. Lett.* **1997**, *281*, 407.
- Zipf, E. C.; Prasad, S. S. *Geophys. Res. Lett.* **1998**, *25*, 4333.
- Cliff, S. S.; Thieme, M. H. *Science* **1997**, *278*, 1774.
- Cliff, S. S.; Brenninkmeijer, C. A. M.; Thieme, M. H. *J. Geophys. Res.* **1999**, *104*, 16171.
- Yung, Y. L.; Miller, C. E. *Science* **1997**, *278*, 1778.
- Miller, C. E.; Yung, Y. L. *Chemosphere: Global Change Sci.* **2000**, *2*, 255.
- Rahn, T.; Zhang, H.; Wahlen, H.; Blake, G. A. *Geophys. Res. Lett.* **1998**, *25*, 4489.
- Rockmann, T.; Brenninkmeijer, C. A. M.; Wollenhaupt, M.; Crowley, J. N.; Crutzen, P. J. *Geophys. Res. Lett.* **2000**, *27*, 1399.
- Turatti, F.; Griffith, D. W. T.; Wilson, S. R.; Rahn, T.; Zhang, H.; Blake, G. A. *Geophys. Res. Lett.* **2000**, *27*, 2489.
- Zhang, H.; Wennberg, P. O.; Wu, V. H.; Blake, G. A. *Geophys. Res. Lett.* **2000**, *27*, 2481.
- Rockmann, T.; Kaiser, J.; Brenninkmeijer, C. A. M.; Crowley, J. N.; Borchers, R.; Brand, W. A.; Crutzen, P. J. *J. Geophys. Res.* **2001**, *106*, 10403.
- Rahn, T.; Wahlen, M. *Science* **1997**, *278*, 1776.
- Griffith, D. W. T.; Toon, G. C.; Sen, B.; Blavier, J. F.; Toth, R. A. *Geophys. Res. Lett.* **2000**, *27*, 2485.
- Anderson, S. M.; Mauersberger, K.; Morton, J. In *Progress and Problems in Atmospheric Chemistry*; Barker, J. R., Ed.; World Scientific: Singapore, 1995.
- Anderson, S. M.; Mauersberger, K.; Morton, J.; Schueler, B. *ACS Symp. Ser.* **1992**, *502*, 155.
- Krankowsky, D.; Lammerzahl, P.; Mauersberger, K. *Geophys. Res. Lett.* **2000**, *27*, 2593 and references therein.
- Krankowsky, D.; Bartecki, F.; Klees, G. G.; Mauersberger, K.; Schellenbach, K.; Stehr, J. *Geophys. Res. Lett.* **1995**, *22*, 1713.
- Johnston, J. C.; Thieme, M. H. *J. Geophys. Res.* **1997**, *102*, 25395.
- Prasad, S. S.; Zipf, E. C. *Chemosphere: Global Change Sci.* **2000**, *2*, 235.
- Rockmann, T.; Kaiser, J.; Crowley, J. N.; Brenninkmeijer, C. A. M.; Crutzen, P. J. *Geophys. Res. Lett.* **2001**, *28*, 503.
- Gaedtke, H.; Glanzer, K.; Hippler, H.; Luther, K.; Troe, J. *Fourteenth Symposium (International) on Combustion*; 1972; p 295.
- Kajimoto, O.; Cvetanovic, R. J. *J. Chem. Phys.* **1976**, *64*, 1005.
- Maric, D.; Burrows, J. P. *J. Photochem. Photobiol. A: Chem.* **1992**, *66*, 291.
- Estupiñán, E. G.; Stickel, R. E.; Wine, P. H. *Chemosphere: Global Change Sci.* **2000**, *2*, 247.
- Estupiñán, E. G.; Stickel, R. E.; Wine, P. H. *Chem. Phys. Lett.* **2001**, *336*, 109.
- Brock, J. C.; Watson, R. T. *Chem. Phys. Lett.* **1980**, *71*, 371.
- Yoshino, K.; Freeman, D. E.; Esmond, J. R.; Parkinson, W. H. *Planet. Space Sci.* **1988**, *36*, 395.
- Barnes, J.; Mauersberger, K. *J. Geophys. Res.* **1987**, *92*, 14861.
- Molina, L. T.; Molina, M. J. *J. Geophys. Res.* **1986**, *91*, 14501.
- Mauersberger, K.; Barnes, K.; Hanson, D.; Morton, J. *Geophys. Res. Lett.* **1986**, *13*, 671.
- Hearn, A. G. *Proc. Phys. Soc. (London)* **1961**, *78*, 932.
- Inn, E. C. Y.; Tanaka, Y. *J. Opt. Soc. Am.* **1953**, *43*, 870.
- Wayne, R. P. *Atmos. Environ.* **1987**, *21*, 1683.
- Ackerman, M. In *Mesospheric Models and Related Experiments*; Fiocco, G., Ed.; Reidel: Dordrecht, Holland, 1971.
- Goody, R. M.; Walshaw, C. D. *Q. J. R. Meteorol. Soc.* **1953**, *79*, 496.
- Harteck, P.; Dondes, S. *J. Chem. Phys.* **1954**, *22*, 758.
- DeMore, W.; Raper, O. F. *J. Chem. Phys.* **1962**, *37*, 2048.
- Norrish, R. G. W.; Wayne, R. P. *Proc. R. Soc. London, Ser. A* **1965**, *288*, 200.
- Katakis, D.; Taube, H. *J. Chem. Phys.* **1962**, *36*, 416.
- Simonaitis, R.; Lissi, E.; Heicklen, J. *J. Geophys. Res.* **1972**, *77*, 4248.
- Hartland, G. V.; Qin, D.; Dai, H.-L. *J. Chem. Phys.* **1995**, *102*, 8677.
- Hartland, G. V.; Qin, D.; Dai, H.-L.; Chen, C. *J. Chem. Phys.* **1997**, *107*, 2890.
- Chimbayo, A.; Toselli, B. M.; Barker, J. R. *J. Chem. Phys.* **1998**, *108*, 2383.
- Noxon, J. F. *J. Chem. Phys.* **1970**, *52*, 1852.
- Biedenkapp, D.; Bair, E. *J. Chem. Phys.* **1970**, *52*, 6119.
- Snelling, D. R. *Can J. Chem.* **1974**, *52*, 257.
- Lee, L. C.; Slanger, T. G. *J. Chem. Phys.* **1978**, *69*, 4053.
- Sander, S. P.; Friedl, R. R.; DeMore, W. B.; Golden, D. M.; Kurylo, M. J.; Hampson, R. F.; Huie, R. E.; Moortgat, G. K.; Ravishankara, A. R.; Kolb, C. E.; Molina, M. J. *Chemical Kinetics and Photochemical Data for Use in Stratospheric Modeling, Evaluation No. 13*; Jet Propulsion Laboratory: Pasadena, CA, 2000.
- Ravishankara, A. R.; Dunlea, E. J.; Blitz, M. A.; Dillon, T. J.; Heard, D. E.; Pilling, M. J.; Strekowski, R. S.; Nicovich, J. M.; Wine, P. H. *Geophys. Res. Lett.*, in press.
- Saxon, R. P.; Slanger, T. G. *J. Geophys. Res.* **1986**, *91*, 9877.
- Tully, J. C. *J. Chem. Phys.* **1974**, *61*, 61.
- Zahr, G. E.; Preston, R. K.; Miller, W. H. *J. Chem. Phys.* **1975**, *62*, 1127.
- Tachikawa, H.; Hamabayashi, T.; Yoshida, H. *J. Phys. Chem.* **1995**, *99*, 16630.
- Wang, H. J.; Cunnold, D. M.; Froidevaux, L.; Russell, J. M. *J. Geophys. Res.* **1999**, *104*, 21629.
- Logan, J. A. *J. Geophys. Res.* **1999**, *104*, 16115.
- Ramaroson, R.; Pirre, M.; Cariolle, D. *Ann. Geophys.* **1992**, *10*, 416.
- Prasad, S. S. *EOS Trans. AGU* **2001**, *82* (47), Fall Mtg. Suppl., Abstract A32B-0057.